Thermodynamics and conformation of polyoxyethylene in aqueous solution under high pressure: 1. Small-angle neutron scattering and densitometric measurements at room temperature

N. Vennemann and M. D. Lechner
Physikalische Chemie, Universität Osnabrück, Barbarastrasse 7, D-4500 Osnabrück, West Germany

and R. C. Oberthür
Institut Laue-Langevin, BP 156X, F-38042 Grenoble, France
(Received 10 November 1986; revised 14 January 1987; accepted 24 January 1987)

Volumetric data of the polyoxyethylene (POE)/water system at 25°C and pressures up to 40 MPa are reported together with small-angle neutron scattering (SANS) measurements of dilute solutions of POE in water at 25°C and pressures up to 200 MPa. The combination of both data is used to interpret the variation of the radius of gyration and the second virial coefficient of POE with pressure by means of existing theories on dilute polymer solutions. This allows the evaluation of the unperturbed dimensions of POE in water at 25°C.

(Keywords: neutron scattering; polyoxyethylene; high pressure; densitometry; conformation)

INTRODUCTION

The influence of pressure on the conformation and interaction of water-soluble macromolecules, especially proteins, other biopolymers and membranes, has recently attracted much attention[1-3]. This is understandable since living organisms have been detected under extreme physical conditions[4], e.g. at the bottom of the deep sea under hydrostatic pressures up to 100 MPa.

The understanding of the conformational stability of biopolymers under such conditions may become a major task for molecular physics. To contribute to an understanding of the variation of conformation and interaction of a polymer in an aqueous environment under high pressure we have chosen the simplest water-soluble polymer, polyoxyethylene (POE), with a repeating unit $-CH_2-CH_2-O-$.

POE is a remarkable polymer in several respects (see ref. 5): it is soluble in water from 0°C to about 100°C and soluble in most organic solvents, although its lower homologue, polyoxymethylene, as well as all its higher homologues, polyoxypropylene, polyoxybutylene, etc., are insoluble in water but soluble in most organic solvents.

Hence, we can hope that, even in the simple case of POE, water will play an important role in the stabilization of its conformation in solution, and that changes in the thermodynamic state of water will lead to changes in the conformation and interaction of this linear polymer, where they are easier to interpret than in the complex case of a protein.

MATERIAL

Polyoxyethylene

The investigated POE was a product from Serva (Heidelberg, Germany) with the specifications $n = 800$–900 monomer units. It was used without further purification. Gel permeation chromatography with a Sephadex G-200 column revealed a small polydispersity ($M_w/M_n < 1.1$). Tentative measurements with high-angle light scattering in water at 25°C yielded a mass-average molar mass M_w between 25 000 and 30 000 g mol^{-1}. The Staudinger index in water at 25°C was $[\eta] = 52.5$ cm^3 g^{-1}. This leads to a molar mass M_η between 35 000 and 60 000 g mol^{-1} according to the different molar mass–viscosity relationships quoted in the literature[5,6].

Water

Light water was bidistilled with a conductivity of 1 to 2 μS cm^{-1}. Heavy water was purchased from Merck (Darmstadt, Germany) with a D_2O content of 99.75% D. Its conductivity was less than 1 μS cm^{-1}.

Solutions

Solutions of POE in water were prepared by weighing first the polymer, then the water into an appropriate vessel. The POE was then allowed to dissolve in the water, supported by shaking the vessel. When the solution was visually homogeneous it was placed in an oven at a temperature of 10 K above the melting point of POE ($T_m = 70$°C) to guarantee the dissolution of any possible remaining crystallites of POE[7,8].

0032-3861/87/101738-11$03.00

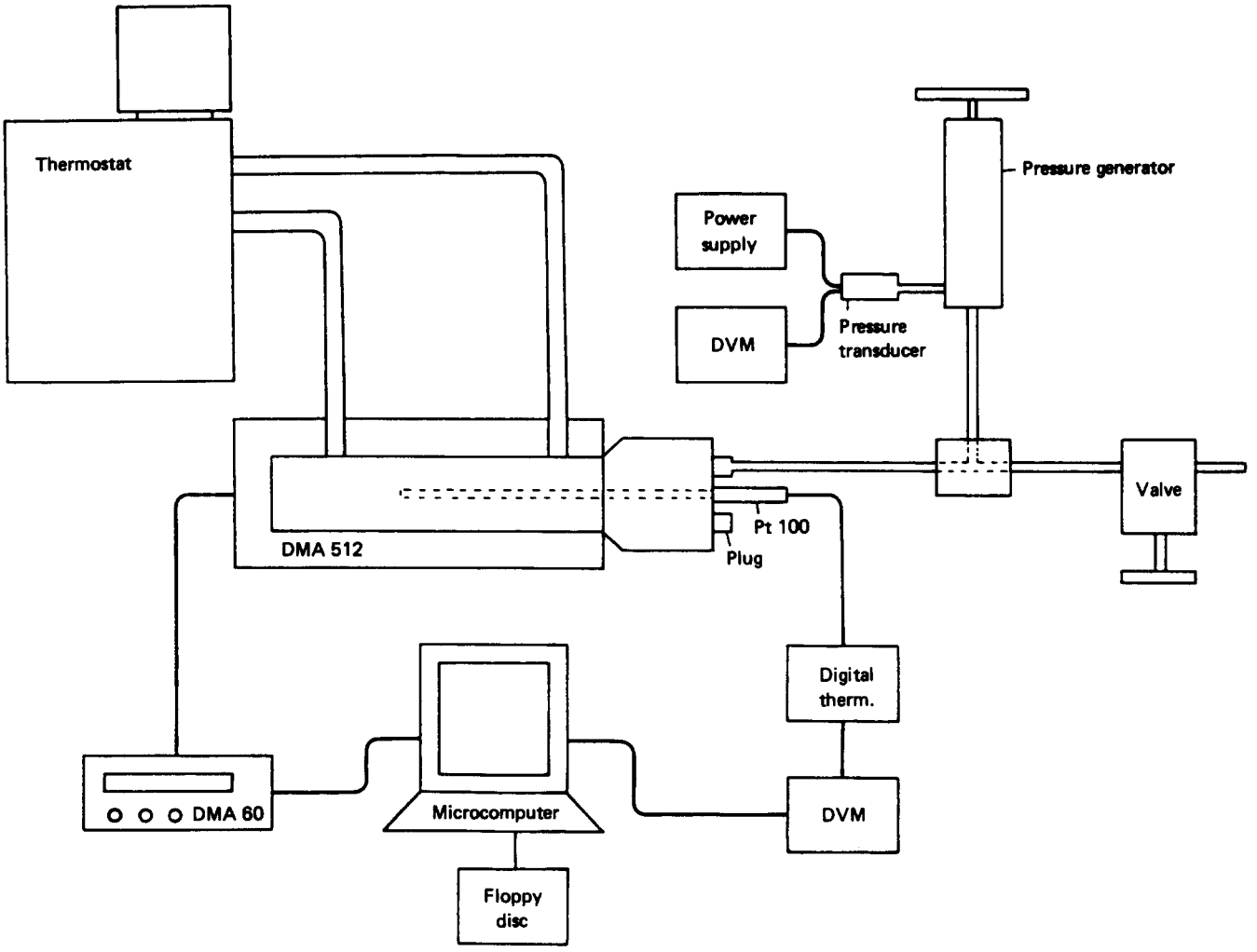

Figure 1 Scheme of the experimental set-up for the densitometric measurements

DENSITOMETRY

Experimental equipment

The density measurements were carried out with a commercially available densitometer of type DMA 512 in combination with the reading unit DMA 60 (both instruments from Anton Paar, Graz, Austria). The densitometer applies the principle of a vibrating tube and has been developed by Kratky and Stabinger *et al.*[9]. The external cell DMA 512 is designed for temperatures and pressures up to 150°C and 40 MPa, respectively. The experimental set-up is shown schematically in *Figure 1*. The temperature of the cell was stabilized by an ultrathermostat within ± 0.01 K. The high-pressure system was obtained from Nova Swiss (Effretikon, Switzerland). The pressure could be measured with a resolution of 0.005 MPa by use of a pressure transducer (type 8206) obtained from Burster (Gernsbach, Germany). The whole system, except for the cell and a connecting tube, was filled with distilled water. The solution/water interface was at a distance of about 20 cm from the beginning of the vibrating tube.

Data evaluation

For a given temperature T and pressure p the density ρ of a liquid in the vibrating tube is determined by

$$\rho = aD^2 - b \tag{1}$$

D is the period of vibration, a and b are constants. Both constants depend on temperature but only b depends on pressure[10]. The dependences of a and b on pressure and temperature were determined by use of bidistilled water and air since their densities are well known over a wide range of pressure and temperature[11,12]. In order to obtain volumetric data of dissolved or dispersed particles, usually not the absolute density values are measured but only the density increment $\Delta\rho$ of the solution with respect to the pure solvent. Measuring the period of vibration of the solvent D_0, and of the solution D, at the same temperature and pressure, $\Delta\rho$ can be determined with high accuracy according to

$$\Delta\rho = a(D^2 - D_0^2) \tag{2}$$

The maximum error in $\Delta\rho$ for the measurements reported here can be estimated to be less than 2×10^{-5} g cm^{-3}. The experimental data of $\Delta\rho$ were used to calculate the molar volume V_m of the solution as well as the apparent specific volume v_2^* of the solute as a function of pressure and composition, represented by x_2, the mole fraction, and w_2, the mass fraction, of the solute:

$$V_m = [M_1(1-x_2) + M_2 x_2]/(\rho_0 + \Delta\rho) \tag{3}$$

$$v_2^* = \{1 - \Delta\rho/[W_2(\rho_0 + \Delta\rho)]\}/\rho_0 \tag{4}$$

where M_1 and M_2 are the molar mass of the solvent

($M_1 = 18.015\ \mathrm{g\ mol^{-1}}$) and of the monomer unit of the solute ($M_2 = 44.053\ \mathrm{g\ mol^{-1}}$), respectively.

Results

In contrast to the scattering experiments, the densitometric study was extended to concentrated solutions. In the dilute range no dependence of the apparent specific volume v_2^* on concentration could be observed within the limits of experimental error (see *Figure 2*).

In general, most of the polymer/solvent systems exhibit a similar behaviour, except for polyelectrolytes where a slight increase of v_2^* with increasing concentration has been observed[13]. From the thermodynamic point of view a constant v_2^* can only be expected in the case of ideal solutions. The constant behaviour of v_2^* in the dilute range in our case, therefore, has to be explained with the limited accuracy of the experimental values.

In order to deduce volume quantities that reflect the interactions between solvent and polymer molecules, the accuracy has to be improved and/or, if that is not possible, the measurements have to be extended to higher concentrations.

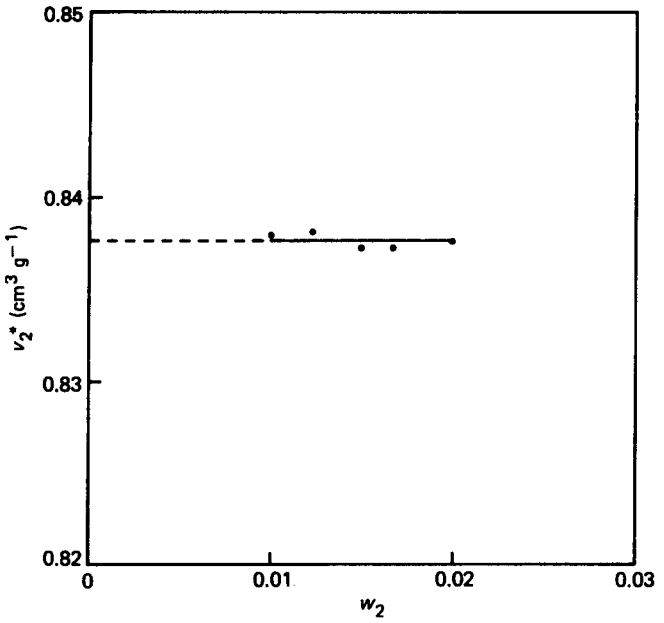

Figure 2 Apparent specific volume v_2^* of POE in H_2O at 25°C and 0 MPa as a function of mass fraction w_2

At this point it is helpful to introduce the thermodynamic excess functions (*Table 1*). A molar excess function is defined as the difference between a real and an ideal mixture, both at the same temperature, pressure and composition. For the molar excess volume V_m^E we get

$$V_m^E = V_m - \sum x_i V_i^\circ \quad (5)$$

with V_i° the molar volumes of the pure components. For binary mixtures the excess functions can be expressed by power series of the mole fraction x_2 (*Table 1*). Guggenheim[14] first derived for the molar Gibbs free energy:

$$G_m^E = x_2(1-x_2)[A + B(2x_2-1) + C(2x_2-1)^2 + \ldots] \quad (6)$$

The coefficients, A, B, C, ... are empirical parameters deduced from experimental data. Because of the term $x_2(1-x_2)$, G_m^E is equal to zero for $x_2 = 0$ and $x_2 = 1$.

A similar relation is obtained for the molar excess volume V_m^E, the pressure derivative of G_m^E:

$$(\partial G_m^E/\partial p) = V_m^E = x_2(1-x_2)[A' + B'(2x_2-1) + C'(2x_2-1) + \ldots] \quad (7)$$

Note that the parameters A, B, C, ... in equation (6) are functions of pressure and temperature and therefore A', B', C', ... in equation (7) and *Table 1* are the corresponding pressure derivatives.

For the evaluation of the excess volumes according to equation (5) the molar volumes V_i° of the pure components have to be known. For that purpose we present volumetric data of the pure polymer measured with the same instrument as the solutions. Problems arise from the fact that the polymer is in the solid state at 25°C. Therefore the measurements were carried out at temperatures above the melting point (70°C). To be sure that no bubbles are inside the vibrating tube, a minimum pressure of 5 MPa was applied.

The inner part of *Table 2* (numbers in italics) contains the experimentally observed densities of liquid POE at several pressures and temperatures. The values placed outside the italic region are obtained by linear extrapolation. At 0 MPa the densities reported in this work agree within 0.5% with the data reported by Simon and Rutherford[15].

The molar volumes of several POE/H_2O solutions at 25°C and at different pressures are presented in *Table 3*. As before, the values from 50 to 100 MPa are obtained by linear extrapolation. The extrapolated values have to be

Table 1 Some volume quantities for binary systems expressed by use of the empirical parameters A' and B' according to equation (6)

	Definition	Empirical expression
Molar volume	$V_m = V/(n_1+n_2)$	$V_m = x_2(1-x_2)[A' + B'(2x_2-1)] + (1-x_2)V_1^\circ + x_2V_2^\circ$
Molar excess volume	$V_m^E = V_m - x_1V_1^\circ - x_2V_2^\circ$	$V_m^E = x_2(1-x_2)[A' + B'(2x_2-1)]$
Partial molar volume	$V_i = (\partial V/\partial n_i)_{T,p,n_{j\neq i}}$	$V_i = V_i^\circ + V_i^E$
Partial molar excess volume	$V_1^E = V_m - x_2(\partial V_m/\partial x_2) - V_1^\circ$	$V_1^E = (A' - 3B')x_2^2 + 4B'x_2^3$
	$V_2^E = V_m - x_1(\partial V_m/\partial x_2) - V_2^\circ$	$V_2^E = A' - B' + x_2(6B' - 2A') + x_2^2(A' - 9B') + B'x_2^3$
Partial molar volume at infinite dilution	$V_1^\infty = \lim_{x_1 \to 0} V_1$	$V_1^\infty = A' + B' + V_1^\circ$
	$V_2^\infty = \lim_{x_2 \to 0} V_2$	$V_2^\infty = A' - B' + V_2^\circ$

used with caution, because the compressibility of liquids is not a constant but decreases with increasing pressure.

An estimate of the extrapolation error can be obtained from a comparison with pure water. Here a linear extrapolation of the densities in the range of 0 to 40 MPa up to 100 MPa leads to a value that is too low by about 0.3%. With increasing pressure the deviation becomes more significant, e.g. 1.2% at 200 MPa. Because of the small estimated deviation up to 100 MPa it seems allowable to calculate excess volumes by use of the extrapolated values as presented in *Tables 2* and *3*.

The molar excess volume V_m^E as a function of the mole fraction x_2 for POE/H_2O at 25°C is shown in *Figure 3* at different pressures. According to equation (7) the experimental values were fitted by use of two parameters A' and B'.

The dependence on pressure of A' and B' is presented in *Figure 4* and can be approximated by:

$$A'/(\text{cm}^3\ \text{mol}^{-1}) = -4.277 + 0.0107p/\text{MPa} \quad (8)$$

$$B'/(\text{cm}^3\ \text{mol}^{-1}) = -1.80 \quad (9)$$

With the equations (8) and (9) and the p–V–T data of the pure components we are able to calculate all volume quantities of the system POE/H_2O at 25°C and any pressure up to 40 MPa and with some caution up to 100 MPa (*Figures 5, 6* and *7*).

It should be noted that the validity of the extrapolated volumetric data is supported by our high-pressure SANS measurements (see next section).

Table 2 Density of pure POE at various temperatures and pressures

	ρ (g cm^{-3})					
P (MPa)	120.3°C	110.6°C	100.7°C	90.0°C	80.0°C	25.0°C
0	*1.0454*	*1.0525*	*1.0602*	*1.0685*	*1.0764*	1.1186
5	*1.0485*	*1.0555*	*1.0632*	*1.0715*	*1.0794*	1.1214
10	*1.0519*	*1.0587*	*1.0662*	*1.0744*	*1.0821*	1.1233
15	*1.0550*	*1.0617*	*1.0691*	*1.0771*	*1.0847*	1.1253
20	*1.0583*	*1.0648*	*1.0721*	*1.0800*	*1.0876*	1.1275
25	*1.0615*	*1.0680*	*1.0751*	*1.0830*	*1.0904*	1.1298
30	*1.0647*	*1.0711*	*1.0782*	*1.0859*	*1.0932*	1.1321
35	*1.0678*	*1.0741*	*1.0811*	*1.0888*	*1.0961*	1.1347
40	*1.0708*	*1.0771*	*1.0841*	*1.0918*	*1.0991*	1.1376
50	1.0774	1.0833	1.0901	1.0975	1.1045	1.1416
60	1.0838	1.0895	1.0961	1.1033	1.1102	1.1462
70	1.0902	1.0957	1.1021	1.1091	1.1158	1.1508
80	1.0965	1.1019	1.1081	1.1149	1.1214	1.1554
90	1.1029	1.1080	1.1140	1.1207	1.1270	1.1600
100	1.1093	1.1142	1.1200	1.1265	1.1327	1.1646

For meaning of italics, see text

SMALL-ANGLE NEUTRON SCATTERING (SANS)

Experimental

The SANS experiments were carried out at the small-angle neutron scattering instrument PACE of the

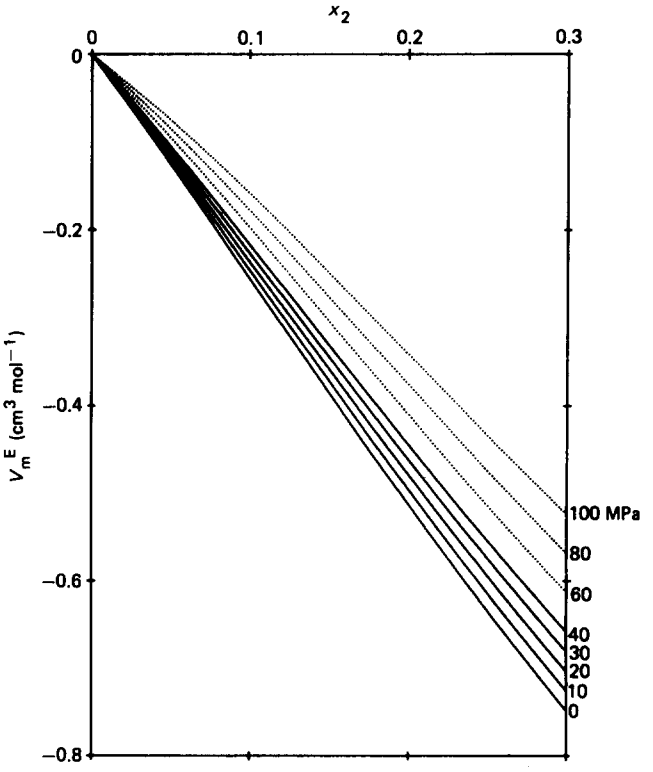

Figure 3 Molar excess volume V_m^E of POE in H_2O at 25°C and different pressures as a function of mole fraction x_2. Full lines: best fits of the experimental values. Dotted lines: best fits of the extrapolated values (see text)

Table 3 Molar volume of several POE/H_2O mixtures at 25°C at various pressures and mole fractions

	V_m (cm^3 mol^{-1})										
x_2	0 MPa	10 MPa	20 MPa	30 MPa	40 MPa	50 MPa	60 MPa	70 MPa	80 MPa	90 MPa	100 MPa
0	*18.068*	*17.988*	*17.910*	*17.834*	*17.760*	17.688	17.618	17.551	17.484	17.420	17.357
0.0085	*18.229*	*18.148*	*18.071*	*17.995*	*17.992*	17.843	17.767	17.690	17.614	17.537	17.460
0.0246	*18.530*	*18.482*	*18.375*	*18.301*	*18.228*	18.148	18.069	17.991	17.912	17.834	17.756
0.0411	*18.841*	*18.764*	*18.688*	*18.616*	*18.542*	18.466	18.392	18.317	18.242	18.168	18.093
0.0405	*18.820*	*18.750*	*18.674*	*18.600*	*18.528*	18.454	18.380	18.307	18.233	18.160	18.086
0.0701	*19.381*	*19.304*	*19.229*	*19.156*	*19.085*	19.009	18.935	18.861	18.788	18.714	18.640
0.1334	*20.556*	*20.481*	*20.408*	*20.337*	*20.267*	20.193	20.121	20.049	19.976	19.904	19.832
0.1496	*20.861*	*20.782*	*20.710*	*20.642*	*20.572*	20.498	20.426	20.354	20.282	20.211	20.139
0.1866	*21.552*	*21.477*	*21.404*	*21.333*	*21.264*	21.190	21.118	21.046	20.974	20.902	20.830
0.2509	*22.770*	*22.692*	*22.617*	*22.545*	*22.474*	22.398	22.324	22.251	22.177	22.103	22.029
0.2914	*23.561*	*23.469*	*23.393*	*23.310*	*23.246*	23.163	23.085	23.007	22.929	22.850	22.772
1	*39.382*	*39.217*	*39.071*	*38.913*	*38.725*	38.589	38.434	38.128	37.977	37.977	37.827

For meaning of italics, see text

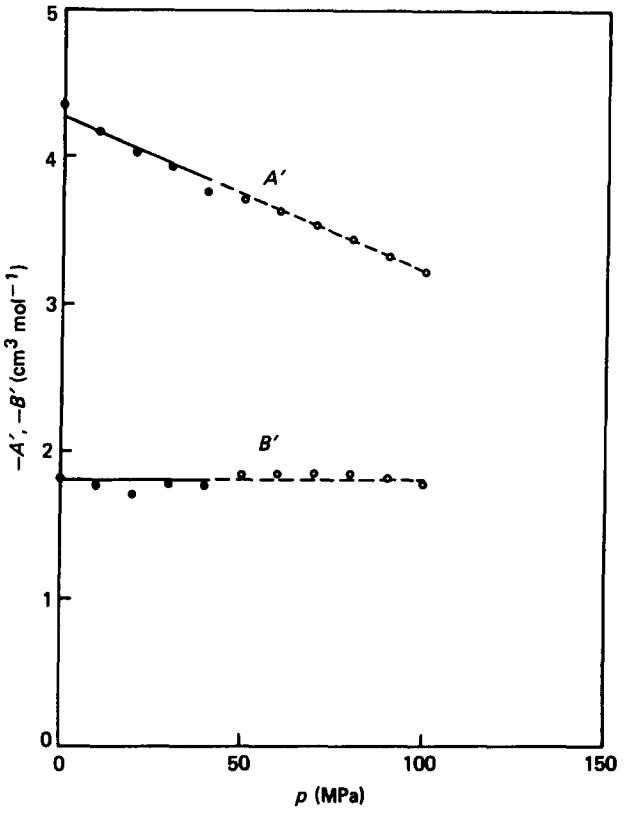

Figure 4 Fit parameters A' and B' according to equation (7) as a function of pressure

Laboratoire Léon Brillouin (LLB) in Saclay, France*. The wavelength and sample–detector distance were 1.2 nm and 2.55 m, respectively.

For neutron scattering experiments under high pressure a special sample cell is required that fulfils both the mechanical and small-angle scattering conditions. Since no commercial high-pressure cell for the requirements of SANS was available, a suitable cell was specially designed and constructed by the mechanical workshop of the University of Osnabrück, Germany, in collaboration with the Institut Laue–Langevin (ILL) in Grenoble, France. A cross section of the cell is presented in *Figure 8*.

The sample volume is placed in the centre of a steel body of 10 cm diameter. The cylindrical sample volume has a diameter of 15 mm and a thickness of 4.5 mm. Two sapphire windows of size 24 mm diameter × 12 mm and 19 mm diameter × 10 mm are held by steel flanges screwed to the steel body. The sealing of the cell is performed by O-rings of gold wire (1 mm diameter) placed between the steel flanges and the windows.

The circular aperture of the entrance window is 12 mm, which is reduced to 10 mm by a cadmium diaphragm to avoid parasitic scattering from the inner walls. The inner part of the steel flange at the exit window is cone-shaped with a cone angle (as indicated in *Figure 8*) of 20°. Thereby the upper value of the observable Q range of the cell is limited. For the measurements reported here the full scattering angle was about 7°.

The experimental set-up is shown schematically in *Figure 9*. The high-pressure system was obtained from Nova Swiss (Effretikon, Switzerland) except for the pressure transducer (type 8212), which was obtained from Burster (Gernsbach, Germany).

The pressure generator and the tubes were filled with D_2O. The filling of the cell with the solution occurred via a connecting tube, from bottom to the top in order to avoid bubbles in the sample volume. The solution/D_2O interface was at a distance of about 20 cm from the cell.

Data evaluation

The scattering behaviour of a solution depends on its thermodynamic state, characterized by the parameters temperature, pressure and composition. In order to separate the influence of the different parameters, two of them must be kept constant. Usually experiments are performed at constant temperature and pressure, where the angular distribution of the scattered intensity for several concentrations of the solute is measured. By subtraction of the background scattering, caused by the solvent, the sample cell, etc., the partial differential scattering cross section of the solute per unit volume $(d\Sigma/d\Omega)_2$ is obtained, if the scattered intensity is normalized to absolute units. According to Zimm[16]

$$Kc/(d\Sigma/d\Omega)_2 = 1/[MP(Q)] + 2A_2c + \ldots \quad (10)$$

where c is the mass concentration, Q is the scattering vector ($|Q| = (4\pi/\lambda)\sin(\theta/2)$, θ = full scattering angle, M is the molar mass of the dissolved particles and A_2 is the second virial coefficient of the osmotic pressure of the

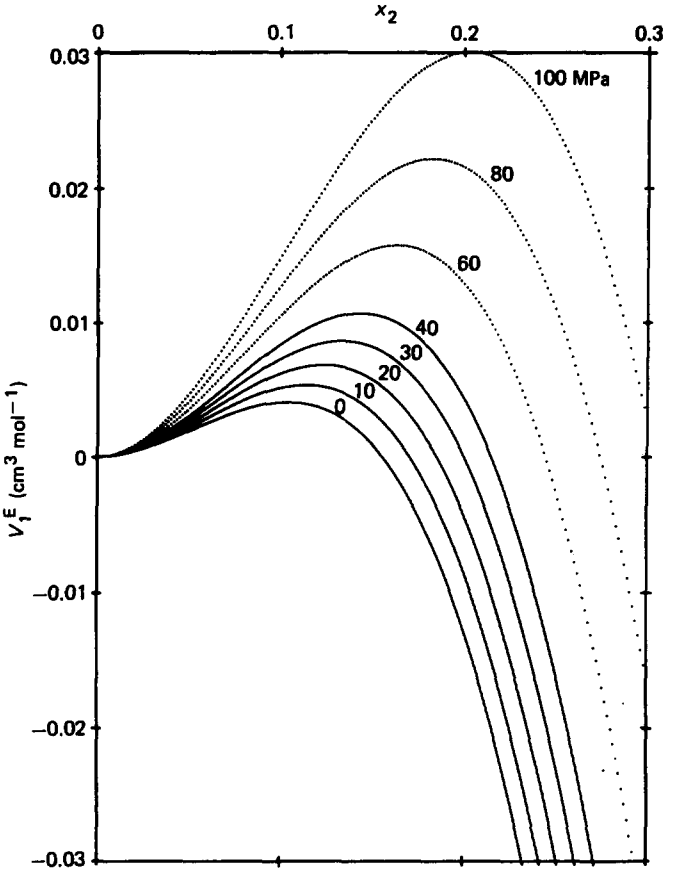

Figure 5 Partial molar excess volume V_1^E of the system POE/H_2O at 25°C and different pressures as a function of mole fraction x_2. Dotted curves indicate extrapolated functions (see text). The functions are calculated by use of the empirical parameters A' and B' (see *Figure 4*)

* Cf. Laboratoire Léon Brillouin, 'Equipements Experimentaux', Saclay, 1982

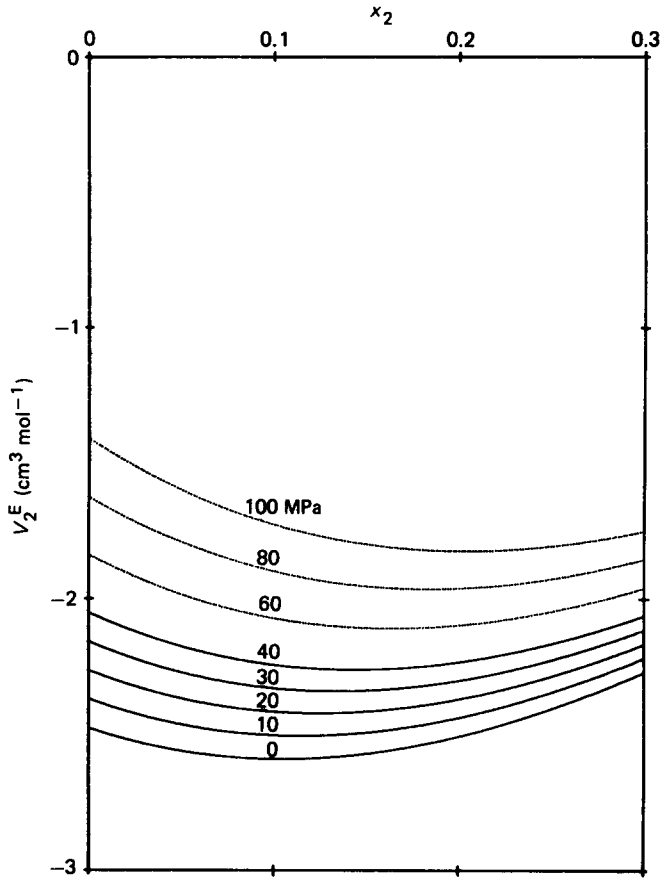

Figure 6 Partial molar excess volume V_2^E of the system POE/H_2O at 25°C and different pressures as a function of mole fraction x_2. Dotted curves indicate extrapolated functions (see text). The functions are calculated by use of the empirical parameters A' and B' (see *Figure 4*)

solution. For dilute solutions all higher virial coefficients are neglected. The single-particle scattering function (structure factor) $P(Q)$ represents the intramolecular part of the scattering cross section, whereas the second term on the right-hand side of equation (10) reflects the intermolecular interferences. The constant K (contrast factor) is determined by the scattering length density increment Δb of the solute

$$K=(\Delta b)^2/N_A \tag{11}$$

where N_A is Avogadro's number and Δb is given by[17]:

$$\Delta b=b_2-b_1\rho_1^\circ v_2^\infty \tag{12}$$

ρ_1° and v_2^∞ being the mass density of the pure solvent and the partial specific volume of the solute at infinite dilution, respectively. The specific scattering lengths of the solvent (D_2O: $b_1=5.767\times10^{10}$ cm g^{-1}) and of the monomer unit of the polymer (C_2H_4O, $b_2=0.5664\times10^{10}$ cm g^{-1}) are obtained from the tabulated atomic scattering length[18] and atomic masses[19].

The scattered intensity of the solvent and of four solutions were measured at 25°C and at three different pressures (0, 100, 200 MPa). In order to normalize the relative intensities I, the incoherent scattering of a 1 mm H_2O sample at 25°C was used as a standard. Taking into account its primary beam transmission T, with respect to the empty beam, each spectrum was corrected for the scattering of the empty cell and then divided by the thickness of the cell, d.

The absolute scattering cross section per unit volume ($d\Sigma/d\Omega$) of the sample is obtained according to

$$(d\Sigma/d\Omega)=(d\Sigma/d\Omega)_w^{1\,mm}[(I_s/T_s-I_{PC}/T_{PC})/d_{PC}]/[(I_w/T_w-I_{WC}/T_{WC})/d_{WC}] \tag{13}$$

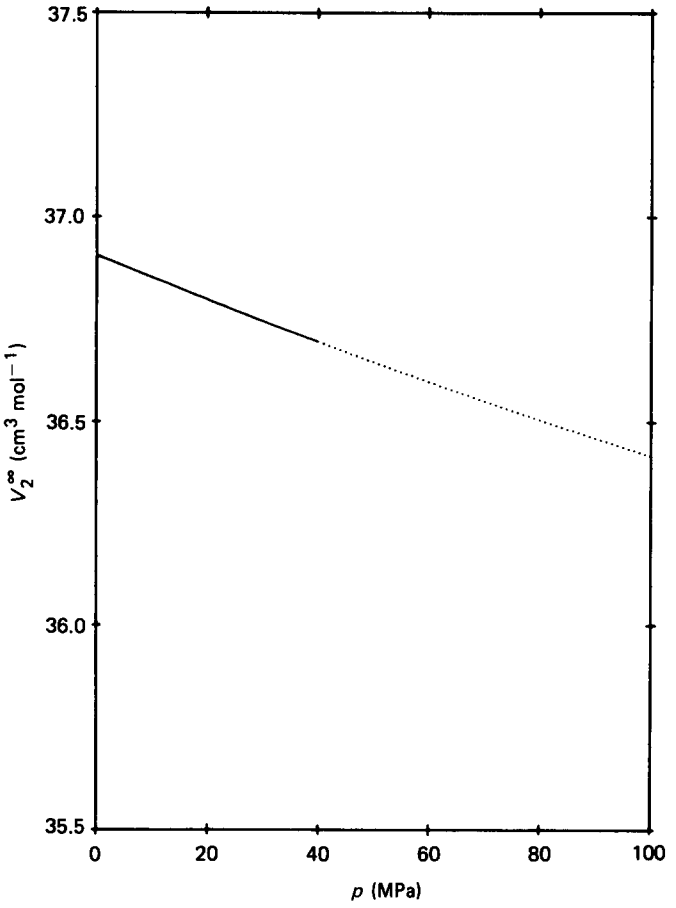

Figure 7 Partial molar volume at infinite dilution V_2^∞ of the system POE/H_2O at 25°C as a function of pressure. The function is calculated by use of the empirical parameters A' and B' (see *Figure 4*)

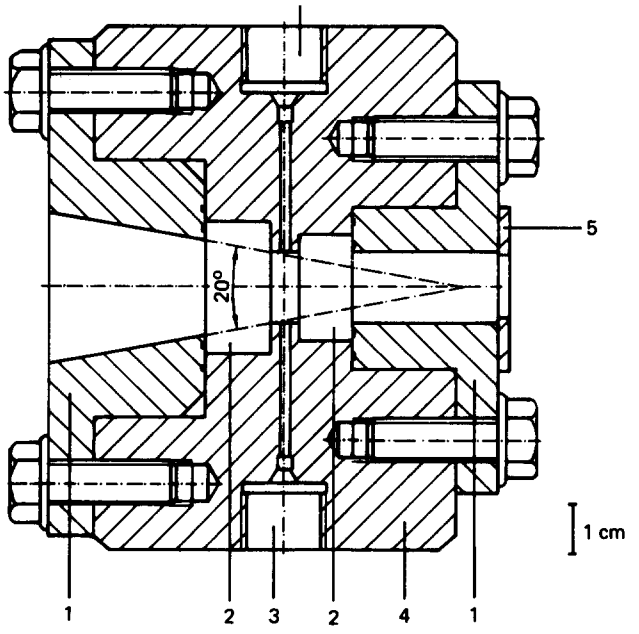

Figure 8 Cross section of the high-pressure cell: 1, steel cap; 2, sapphire windows; 3, pressure connection; 4, steel body; 5, cadmium diaphragm

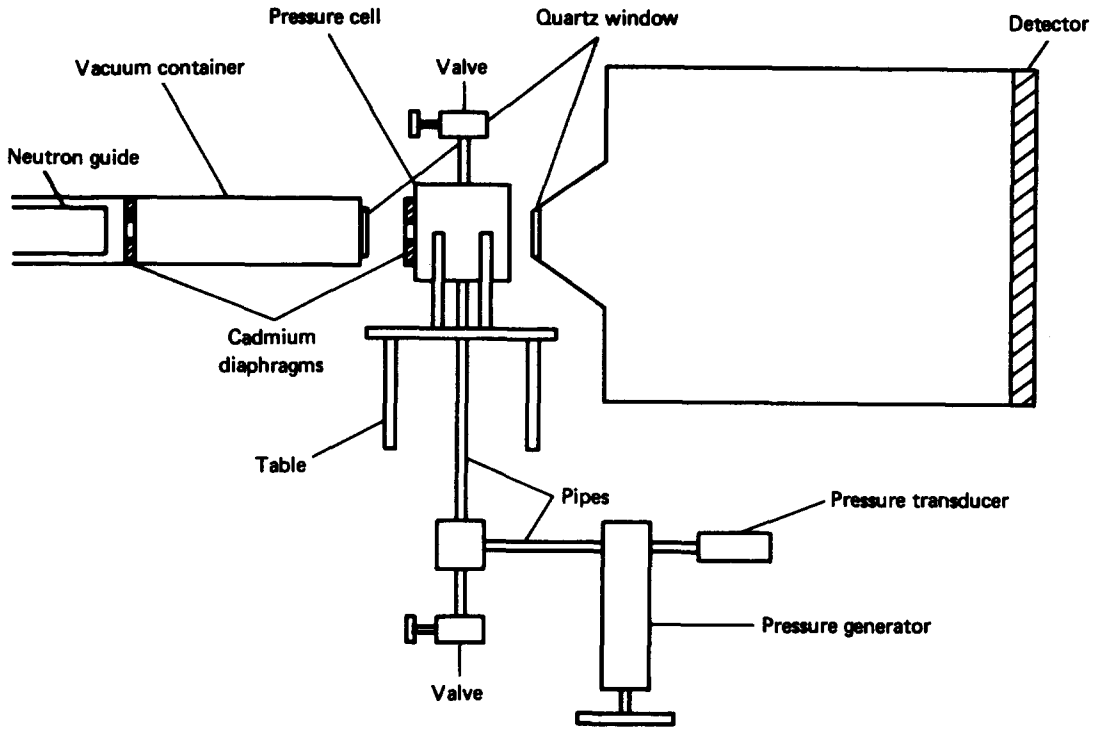

Figure 9 Scheme of the experimental set-up for the SANS experiments

The subscripts PC and WC indicate the empty pressure cell and the empty water cell, respectively. The absolute scattering cross section of a 1 mm H_2O sample $(d\Sigma/d\Omega)_w^{1\,mm}$ was calculated by the empirical expression[20]:

$$(d\Sigma/d\Omega)_w^{1\,mm} = \exp[-0.028 + 0.285 \ln(\lambda/nm) + 0.072 \ln^2(\lambda/nm)] \quad cm^{-1} \quad (14)$$

Subtraction of the scattering cross section of the pure solvent $(d\Sigma/d\Omega)_1^\circ$ from that of the solution yields the scattering of the solute:

$$(d\Sigma/d\Omega)_2 = (d\Sigma/d\Omega) - (1 - c/\rho_1^\circ)(d\Sigma/d\Omega)_1^\circ \quad (15)$$

Results

The scattering data, treated as described above, are represented in *Figures 10a–c* in so-called square-root plots. Here, in contrast to a Zimm plot, the term $[Kc/(d\Sigma/d\Omega)_2]^{1/2}$ is plotted against $Q^2 + \text{constant} \times c$. Extrapolation to zero scattering angle ($Q = 0$) yields a straight line with slope $A_2\sqrt{M}$ that intercepts the ordinate at $1/\sqrt{M}$. From the extrapolation to zero concentration the scattering curve of an isolated polymer coil is obtained. It is obvious from equation (10) that

$$\lim_{\substack{Q\to 0 \\ c\to 0}} (d\Sigma/d\Omega)_2/(Kc) = M \quad (16)$$

Hence the molar mass M is obtained from the value of the single-particle scattering curve at $Q = 0$ as well.

It is noteworthy that synthetic polymers are polydisperse with respect to molar mass so that the quantities obtained by scattering experiments are mean values. For the molar mass M the mass average M_w is obtained, whereas for the structure factor P and the second virial coefficient A_2 we obtain the z averages P_z and $(A_2)_{z,z}$ (ref. 21). However, in the following we neglect all effects of polydispersity, since $M_w/M_n < 1.1$ for our sample.

For nearly monodisperse samples the mean square radius of gyration $\langle R^2 \rangle$ can best be calculated from the initial slope of the single-particle scattering curve in a square-root plot (cf. ref. 22, *Figure 2*):

$$\lim_{c\to 0} [Kc/(d\Sigma/d\Omega)_2]^{1/2} = M^{-1/2}[1 + (\langle R^2 \rangle/6)Q^2 + \ldots] \quad (17)$$

The structural and thermodynamic parameters obtained from the scattering data as presented in *Figure 10* are tabulated in *Table 4*. The values presented in the first three columns are directly deduced from the scattering data. Introducing the volumetric data for the solvent (ρ_1°) and the solute (v_2^∞, see section on 'Densitometry'), the molar mass M and the second virial coefficient A_2 can be calculated.

It should be noted that the value of v_2^∞ (see *Figure 7*) for 100 MPa is a result of an extrapolation as described above. The good agreement of the molar mass for the measurements at 0 and 100 MPa supports the validity of the extrapolation. For the measurements at 200 MPa the molar mass $M = 19 \times 10^3$ g mol^{-1} was used to calculate A_2.

The radii of gyration in *Table 4* are not deduced from the initial slopes of the square-root plots but are obtained by least-squares fits of the whole scattering curve using an empirical relation for the structure factor of an expanded coil[23]:

$$P(Q) = [2(e^{-x} + x - 1)/x^2][2 \arctan(25\pi/x)]^{-0.15} \quad (18)$$

with $x = \langle R^2 \rangle Q^2$.

In *Figures 11a–c* the experimental data are presented together with the best fit of equation (18) in double logarithmic plots of $P(Q)$ against $Q\langle R^2 \rangle^{1/2}$. If we fit the experimental data with the structure factor of an

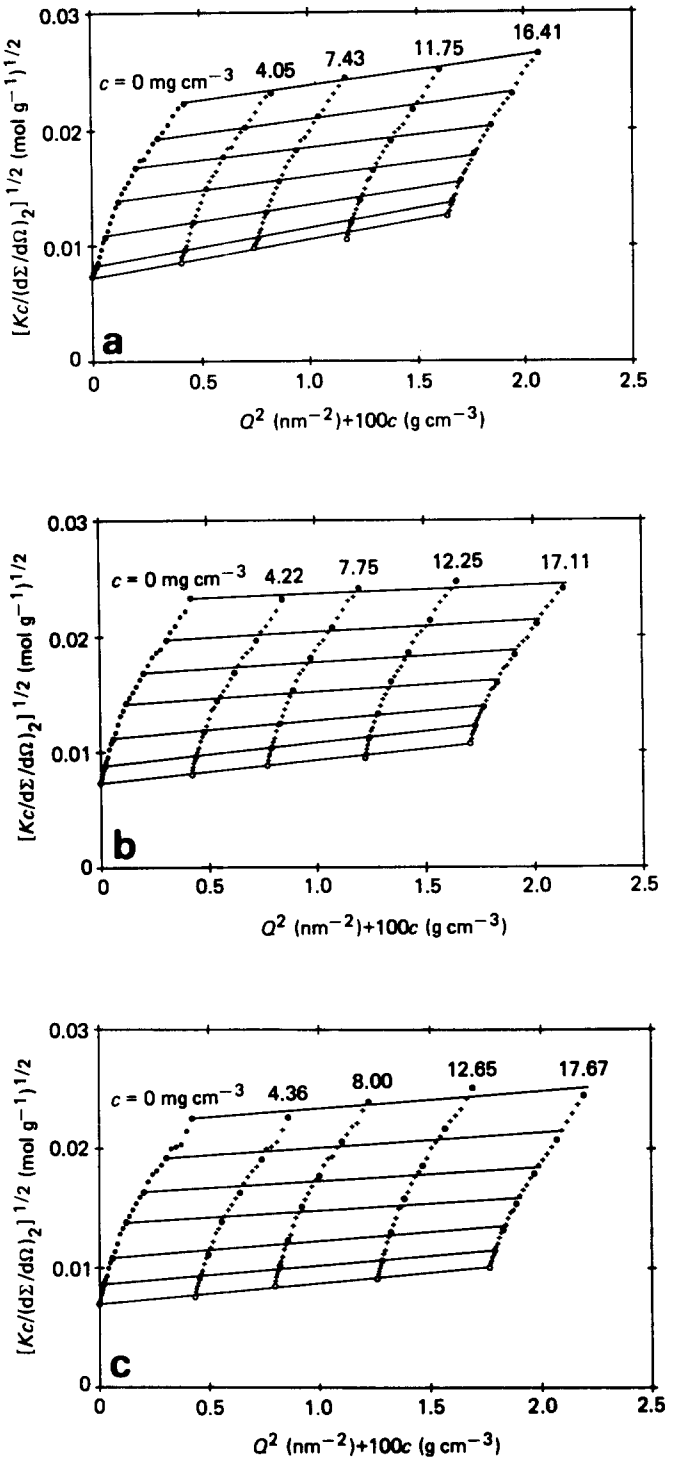

Figure 10 Square-root plots of SANS data of the system POE/D_2O at 25°C: (a) at normal pressure (0 MPa); (b) at 100 MPa; and (c) at 200 MPa; +, measured values; ○, extrapolated values

unperturbed Gaussian coil, a more significant deviation in the range $\langle R^2\rangle^{1/2}Q > 2$ appears.

DISCUSSION

The scattered intensity of a solution is affected by intra- and intermolecular interferences; both are influenced by the thermodynamic state of the solution. The absolute value of the intramolecular part of the scattering cross section is proportional to the molar mass M of the scattering particle and to the contrast factor (see equation (12)). For given scattering lengths of the solvent and the solute the contrast factor is determined by the pressure derivatives of the chemical potentials at infinite dilution:

$$\lim_{x_2\to 0}(\partial\mu_1/\partial p)_T = V_1^0 \tag{19}$$

$$\lim_{x_2\to 0}(\partial\mu_2/\partial p)_T = V_2^\infty \tag{20}$$

Expressed by the excess chemical potentials we obtain:

$$\lim_{x_2\to 0}(\partial\mu_1^E/\partial p)_T = V_1^E = 0 \quad \text{(cf. } \textit{Figure 5}\text{)} \tag{21}$$

$$\lim_{x_2\to 0}(\partial\mu_2^E/\partial p)_T = V_2^E \quad \text{(cf. } \textit{Figure 6}\text{)} \tag{22}$$

which means that V_2^∞ can be substantially different from the corresponding value of the pure substance.

From Zimm's equation (10) it is obvious that the intermolecular interferences, related to the osmotic pressure π, are reflected in the thermodynamic properties as well. In general π can be expressed by the chemical potential of the solvent:

$$\pi = -(\mu_1-\mu_1^\circ)/V_1 = -(\mu_1^{id}-\mu_1^\circ)/V_1 - \mu_1^E/V_1 \tag{23}$$

$$\mu_1^{id} = \mu_1^\circ + RT\ln x_1$$

Comparison with the virial expansion

$$\pi = RTc/M + RTA_2c^2 + RTA_3c^3 + \ldots \tag{24}$$

leads to a relation between A_2 and μ_1^E if, as in the case of low concentrations, higher virial coefficients are neglected:

$$-\mu_1^E = A_2RTV_1c^2 \approx A_2RTM_2^2x_2^2/V_1 \tag{25}$$

The non-ideal behaviour of the solution must have an effect on every other thermodynamic quantity, especially on the excess volumes, which are related to the chemical potentials by

$$V_1^E = (\partial\mu_1^E/\partial p)_T \tag{26}$$

$$V_2^E = (\partial\mu_2^E/\partial p)_T \tag{27}$$

Table 4 Structural and thermodynamic parameters of the system POE/D_2O at 25°C obtained by SANS

P (MPa)	$\lim_{\substack{c\to 0\\ Q\to 0}}(d\Sigma/d\Omega)_2/c$ (cm^2 g^{-1})	$\langle R^2\rangle^{1/2}$ (nm)	A_2M (cm^3 g^{-1})	v_2^∞ (cm^3 g^{-1})	ρ_1° (g cm^{-3})	M_w (g mol^{-1})	A_2 (m^3 mol kg^{-2})
0	76.5	7.3±0.2	49.4	0.838±0.001	1.1044	(20±2)×10^3	(2.4±0.2)×10^{-3}
100	71.3	7.0±0.2	28.7	0.820[a]±0.01	1.1509	(18±2)×10^3	(1.6±0.2)×10^{-3}
200	72.3	6.9±0.2	23.8		1.1877	(19×10^3)	(1.3±0.2)×10^{-3}

[a] Extrapolated value (see text)

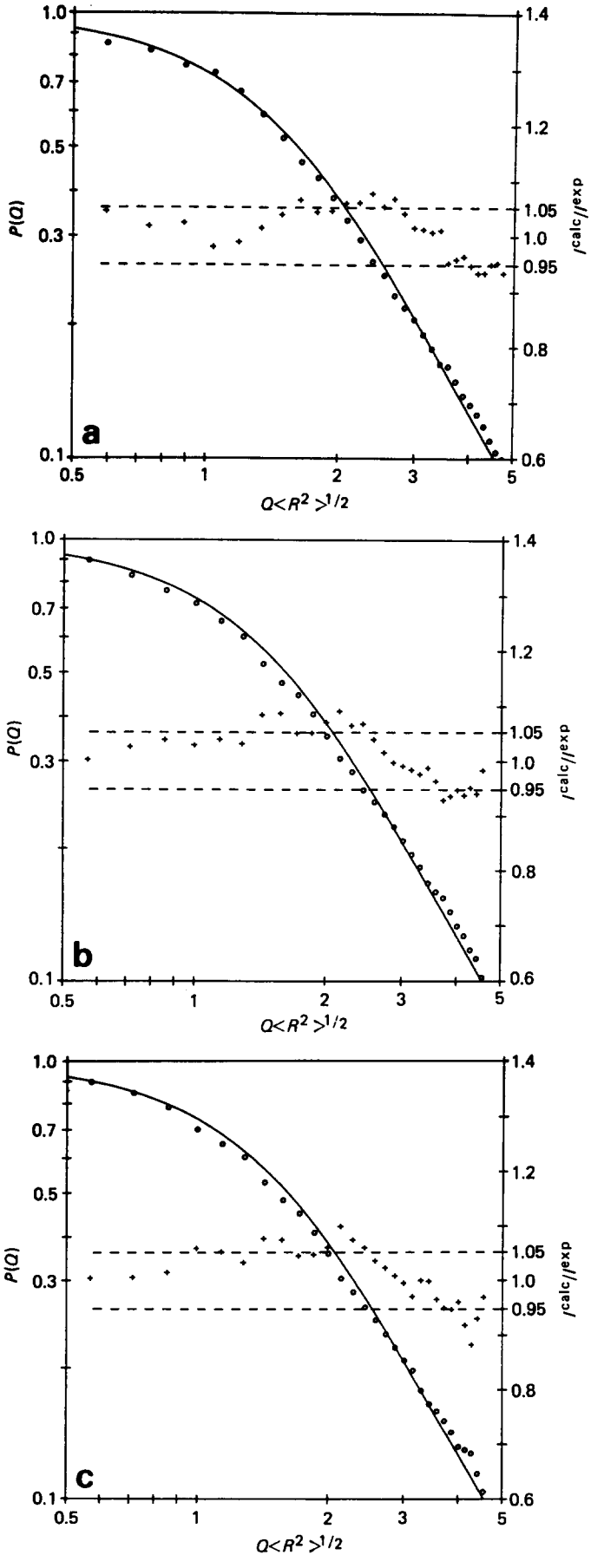

Figure 11 Left-hand scales: structure factor $P(Q)$ (full curve) of POE in D_2O according to equation (18) and measured values (open circles) as a function of $Q\langle R^2\rangle^{1/2}$. Right-hand scales: relative deviation of calculated (I^{calc}) and experimental (I^{exp}) values. (a) At normal pressure (0 MPa); (b) at 100 MPa; (c) at 200 MPa

After differentiation of equation (25) in combination with equation (26), a general relation for the pressure dependence of the second virial coefficient is obtained[24]:

$$V_1^E = (M_2^2 RTx_2^2/V_1)[-(\partial A_2/\partial p)_T - \beta_T A_2] \quad (28a)$$

or

$$V_1^E = V_1 RTc^2[-(\partial A_2/\partial p)_T - \beta_T A_2] \quad (28b)$$

with β_T the isothermal compressibility of the solvent. For binary systems all volume quantities are determined by V_1^E, because of the Gibbs–Duhem theorem. Obviously the dependence of V_1^E on the concentration is reflected in the pressure dependence of A_2, and vice versa. It is interesting to note that at ideal osmotic pressure ($A_2 = 0$) the solution generally can exhibit non-ideal behaviour ($V_1^E \neq 0$) if the term $\partial A_2/\partial p$ is not equal to zero.

The preceding general relations between the scattering of neutrons by dilute solutions and the thermodynamic functions can be summarized in the following diagram:

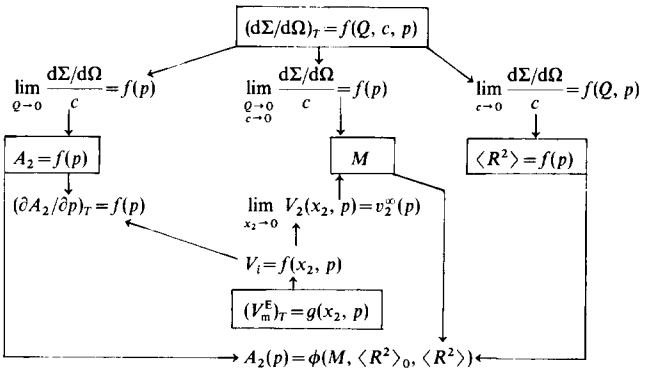

From the diagram it is obvious that the thermodynamic state of the system, fully described by the volume as a function of pressure, temperature and composition, directly acts on the zero-angle scattering ($Q \to 0$) of the solution. For higher Q values, however, where interparticle interferences become negligible, the scattering is dominated by the conformation of a single chain and no simple relations between scattering and thermodynamic data can be expected.

A comparison of zero-angle scattering and volumetric data is offered by equation (28). V_1^E as a function of pressure and composition is determined by the densitometric measurements. Hence, A_2 as a function of pressure can be calculated if an initial value is known. Using the relation for V_1^E, as presented in *Table 1*, equation (28a) becomes

$$A' - 3B' = M^2 RT/V_1[-(\partial A_2/\partial p)_T - \beta_T A_2] \quad (29)$$

when the term with x_2^3 is neglected.

The pressure dependence of A' and B' was determined in the range 0–40 MPa and is given approximately by equations (8) and (9), respectively. Taking into account that V_1° and β_T are functions of pressure as well[11], the differential equation (29) can be solved numerically. In *Figure 12*, A_2 at 25°C of POE in water is plotted against pressure, as calculated by equation (29) with the initial value $A_2 = 2.4 \times 10^{-3}$ cm^3 mol g^{-2} at $p = 0$ MPa.

The values of A_2 observed by SANS, as indicated in *Figure 12*, agree within the limits of experimental error.

Since the same intersegmental forces act on both the

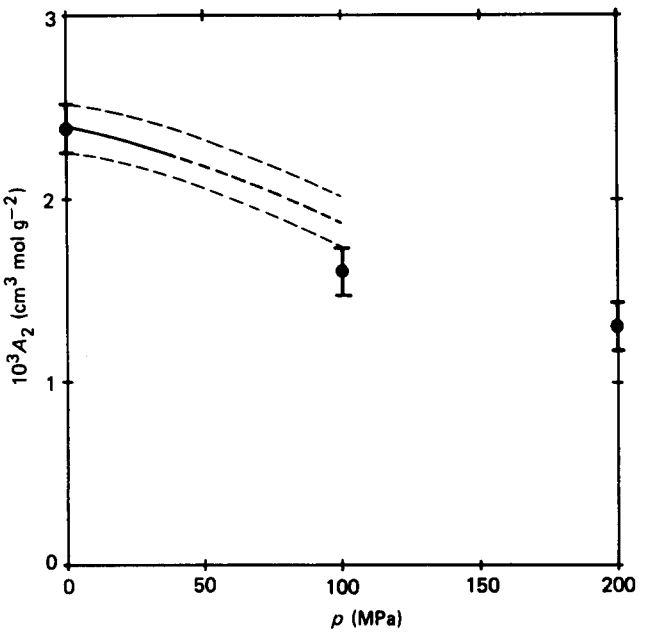

Figure 12 Second virial coefficient A_2 of the system POE/water at 25°C as a function of pressure. Full circles: observed by SANS for POE/D_2O. Full curve: as deduced from volume data for POE/H_2O (see text). Broken curves: as full curve, but by use of extrapolated data

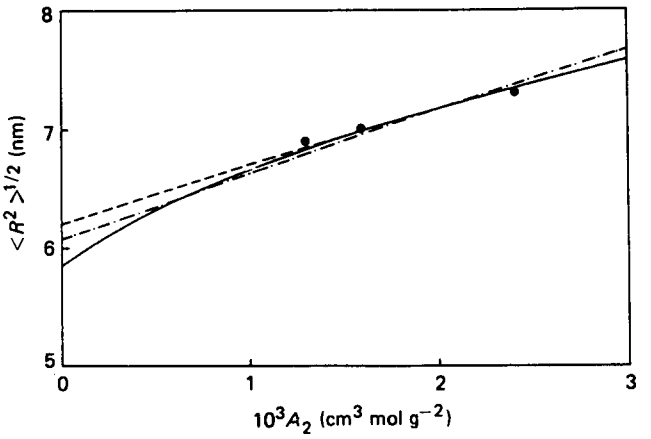

Figure 13 Mean square radius of gyration $\langle R^2\rangle^{1/2}$ as a function of the second virial coefficient A_2 for the system POE/D_2O: ●, experimental values; ——, calculated by theory (i); - - - -, calculated by theory (ii); — · —, calculated by theory (iii) (see text)

intra- and intermolecular interactions of a macromolecule in solution (cf. ref. 22, figure 3b) a relationship must exist between the coil expansion as reflected on the radius of gyration of a perturbed coil and its pair correlation as reflected on its second virial coefficient. Yamakawa has summarized existing theories on this subject[21]:

(i) Original Flory–Krigbaum–Orofino theory

$$A_2(p)=\text{constant}\times\langle R^2\rangle^{3/2}(p) \times 0.435\ln\{1+0.885[\alpha^2(p)-1]\} \quad (30)$$

(ii) Modified Flory–Krigbaum–Orofino theory

$$A_2(p)=\text{constant}\times\langle R^2\rangle^{3/2}(p) \times 0.175\ln\{1+4.49[\alpha^2(p)-1]\} \quad (31)$$

(iii) Kurata–Yamakawa/Yamakawa–Tanaka theory

$$A_2(p)=\text{constant}\times\langle R^2\rangle^{3/2}(p)0.547[1-\{1+0.646 \times[(\alpha^2(p)-0.541)/0.459]^{2.17}-1\}/\alpha^3(p)]^{-0.468}$$

with constant $=4\pi^{3/2}N_A/M^2$ and $\alpha^2(p)=\langle R^2\rangle(p)/\langle R^2\rangle_0$ where $\langle R^2\rangle_0$ is the radius of gyration of the corresponding unperturbed polymer coil of molar mass M.

Comparison of these theories with the experimental data is shown in *Figure 13*.

For the unperturbed dimension of the POE coil in water at 25°C we obtain $\langle R^2\rangle^{1/2}=5.9$ nm, 6.2 nm and 6.1 nm, respectively. This yields with $M=19\,000$ g mol^{-1} values for $(\langle R^2\rangle_0/M)^{1/2}=0.043$ nm (mol g^{-1})$^{1/2}$, 0.045 nm (mol g^{-1})$^{1/2}$ and 0.044 nm (mol g^{-1})$^{1/2}$, respectively. These values may be compared with corresponding data on POE in the melt as obtained from SANS, where 0.045 nm (mol g^{-1})$^{1/2}$ is reported by Allen[25], 0.047 nm (mol g^{-1})$^{1/2}$ by Allen and Maconnachie[26] and 0.041 nm (mol g^{-1})$^{1/2}$ by Kugler[27]. The characteristic ratio $C_\infty=4.0$ given by Flory[28] corresponds to $(\langle R^2\rangle_0/M)^{1/2}=0.031$ nm (mol g^{-1})$^{1/2}$, whereas recent results[29] from viscosimetric data on POE in water at different temperature and ambient pressure yield a value of 0.036 nm (mol g^{-1})$^{1/2}$ at 25°C.

We can conclude that existing theories on conformation of expanded linear chain molecules adequately explain the behaviour of POE in water at room temperature as a function of pressure.

ACKNOWLEDGEMENTS

We gratefully acknowledge the assistance of J.-P. Cotton from the Laboratoire Léon Brillouin, Gif-sur-Yvette, in the performance of the small-angle neutron scattering experiments. Financial support of the 'Deutsche Forschungsgemeinschaft' and the 'Fonds der Chemischen Industrie' is gratefully acknowledged.

REFERENCES

1 Morild, E. *Adv. Protein Chem.* 1981, **34**, 93
2 Weber, G. and Drickamer, H. G. *Q. Rev. Biophys.* 1983, **16**, 89
3 Braganza, L. F. and Worcester, D. L. *Biochemistry* 1986, **25**, 2591
4 Jaenicke, R. *Annu. Rev. Biophys. Bioeng.* 1981, **10**, 1
5 Molyneux, P. in 'Water', Vol. 4, 'Aqueous Solutions of Amphiphiles and Macromolecules' (Ed. F. Franks), Plenum Press, New York, 1975, Ch. 7
6 Bailey, Jr, F. E. and Koleske, J. V. 'Poly(ethylene oxide)', Academic Press, New York, 1976
7 Strazielle, C. *Makromol. Chem.* 1968, **119**, 50
8 Polik, W. F. and Burchard, W. *Macromolecules* 1983, **16**, 978
9 Kratky, O., Leopold, H. and Stabinger, H. *Z. Angew. Phys.* 1969, **27**, 273
10 Stabinger, H. and Rakusch, U., Messtechnik-Nachrichten (Internal Publication of 'Institut für Messtechnik') No. 5, Forschungszentrum Graz, Austria, 1983
11 Chen, C.-T., Fine, R. A. and Millero, F. J. *J. Chem. Phys.* 1977, **66**, 2142
12 Kohlrausch, F. 'Praktische Physik', 22nd Edn, Verlag B.G. Teubner, Stuttgart, 1968, Vol. 3, p. 40
13 Tondre, C. and Zana, R. J. *Phys. Chem.* 1972, **76**, 3451
14 Guggenheim, E. A. *Trans. Faraday Soc.* 1937, **33**, 151
15 Simon, F. T. and Rutherford, Jr, J. M. *J. Appl. Phys.* 1961, **35**, 82
16 Zimm, B. H. *J. Chem. Phys.* 1948, **16**, 1099
17 Cotton, J.-P. and Benoit, H. *J. Physique* 1975, **36**, 905
18 Koester, L. and Steyerl, A. in 'Neutron Physics', Springer, Berlin, 1977
19 'Handbook of Chemistry and Physics' (Ed. R. C. Weast), 57th Edn., CRC Press, Cleveland, Ohio
20 Oberthür, R. C., ILL Internal Report (in preparation)

21 Yamakawa, A., 'Modern Theory of Polymer Solutions', Harper and Row, New York, 1971
22 Kirste, R. G. and Oberthür, R. C., in 'Small Angle X-ray Scattering' (Ed. O. Glatter and O. Kratky), Academic Press, London, 1982, Ch. 12
23 Oberthür, R. C., Ragnetti, M. and Rahlwes, D. (in preparation)
24 Lechner, M. D., Schulz, G. V. and Wolf, B. A. *J. Colloid Interface Sci.* 1972, **39**, 462
25 Allen, G. *Proc. R. Soc. Lond. A* 1976, **351**, 381
26 Allen, G. and Maconnachie, A. *Br. Polym. J.* 1977, **9**, 184
27 Kugler, J. personal communication
28 Flory, P. J. 'Statistical Mechanics of Chain Molecules', Interscience, New York, 1969
29 Gregory, P. and Huglin, M. B. *Makromol. Chem.* 1986, **187**, 1745